BRAIN
A JOURNAL OF NEUROLOGY

Loss and reorganization of calretinin-containing interneurons in the epileptic human hippocampus

Kinga Tóth,[1] Loránd Erőss,[2] János Vajda,[2] Péter Halász,[3] Tamás F. Freund[1] and Zsófia Maglóczky[1]

1 Institute of Experimental Medicine, Hungarian Academy of Sciences, H-1083 Budapest, Hungary
2 National Institute of Neuroscience, H-1145 Budapest, Hungary
3 National Institute of Psychiatry and Neurology, Epilepsy Centre, H-1021 Budapest, Hungary

Correspondence to: Zsófia Maglóczky,
Institute of Experimental Medicine,
Hungarian Academy of Sciences,
Szigony utca 43, H-1083 Budapest, Hungary
E-mail: zmagloczky@koki.hu

Calretinin is expressed mainly in interneurons that specialize to innervate either principal cell dendrites or other interneurons in the human hippocampus. Calretinin-containing cells were shown to be vulnerable in animal models of ischaemia and epilepsy. In the human hippocampus, controversial data were published regarding their sensitivity in epilepsy. Therefore we aimed to reveal the fate of this cell type in human epileptic hippocampi. Surgically removed hippocampi of patients with drug-resistant temporal lobe epileptic ($n = 44$) were examined and compared to control ($n = 8$) samples with different post-mortem delays. The samples were immunostained for calretinin and the changes in the distribution, density and synaptic target selectivity of calretinin-positive cells were analysed. Control samples with post-mortem delays longer than 8h resulted in a reduced number of immunolabelled cells compared to controls with short post-mortem delay. The number of calretinin-positive cells in the epileptic tissue was considerably decreased in correlation with the severity of principal cell loss. Preserved cells had segmented and shortened dendrites. Electron microscopic examination revealed that in controls, 23% of the calretinin-positive interneuronal terminals targeted calretinin-positive dendrites, whereas in the epileptic samples it was reduced to 3–5%. The number of contacts between calretinin-positive dendrites also dropped. The present quantitative data suggest that calretinin-containing cells in the human hippocampus are highly vulnerable, thus inhibition mediated by dendritic inhibitory cells and their synchronization by interneuron-specific interneurons may be impaired in epilepsy. We hypothesize that reorganization of the interneuron-selective cells may be implicated in the occurrence of seizures in non-sclerotic patients, where the majority of principal and non-principal cells are preserved.

Introduction

Changes of hippocampal gamma-aminobutyric acid (GABA) interneuronal circuits are known to play a central role in epileptogenesis (Houser, 1991, 1999; Esclapez and Houser, 1999; Loup *et al.*, 2000; Cossart *et al.*, 2001; Magloczky and Freund, 2005). Although the majority of non-principal neurons seem to be resistant and are present in large numbers in the epileptic human hippocampus (Babb *et al.*, 1989; Sloviter *et al.*, 1991), the selective loss of some interneuron types has also been reported

(de Lanerolle *et al.*, 1988, 1989; Magloczky *et al.*, 2000). A subset of GABAergic inhibitory cells containing calretinin was shown to be vulnerable to ischaemic and epileptic injury both in animal models (Freund and Magloczky, 1993; Magloczky and Freund, 1993; Andre *et al.*, 2001; Slezia *et al.*, 2004; van Vliet *et al.*, 2004; Tang *et al.*, 2006) and humans (Magloczky *et al.*, 2000; Suckling *et al.*, 2000).

Calretinin was found exclusively in non-principal cells in the hippocampus, both in animals and humans (Jacobowitz and Winsky, 1991; Gulyas *et al.*, 1992; Miettinen *et al.*, 1992; Resibois and Rogers, 1992; Seress *et al.*, 1993b; Nitsch and Ohm, 1995). Beside the large amount of calretinin-positive interneurons, there are also a few persisting Cajal–Retzius cells that also show calretinin immunoreactivity (Abraham and Meyer, 2003). The distribution and morphology of calretinin-positive interneurons in the human hippocampus (Urban *et al.*, 2002) were found to be different from those of the rat (Gulyas *et al.*, 1992; Miettinen *et al.*, 1992; Nitsch and Ohm, 1995).

Previous studies described that in the rat CA1 region, calretinin-containing cells selectively terminate on interneurons (Gulyas *et al.*, 1996), mostly those that contain calbindin, and are responsible for the inhibitory control of excitatory synaptic input of principal cell dendrites. In the human hippocampus, calretinin-containing cells are heterogeneous in terms of target selectivity. They all seem to participate primarily in the innervation of other interneurons, and to some extent principal cell dendrites as well (Urban *et al.*, 2002).

Dendritic inhibitory interneurons in the hippocampus can efficiently prevent the generation of dendritic calcium spikes and thereby limit synaptic plasticity, but only if they fire in concert (Miles *et al.*, 1996). The well-studied somatostatin- and neuropeptide Y-containing dendritic inhibitory cells were shown to be sensitive to epilepsy (de Lanerolle *et al.*, 1988; Sundstrom *et al.*, 2001), which may partially explain the loss of dendritic inhibition in epileptic samples (Cossart *et al.*, 2001). However, these cells displayed a remarkable sprouting both in animal models and human epileptic samples (de Lanerolle *et al.*, 1989), and other dendritic inhibitory cells containing calbindin are well preserved (Sloviter *et al.*, 1991) and also show sprouting (Wittner *et al.*, 2002). In spite of this survival and sprouting, dendritic inhibition is not effective in epilepsy (Cossart *et al.*, 2001), which means that other factors are also likely to be involved.

The calretinin-containing inhibitory cells are probably responsible for the synchronization of dendritic inhibitory cells (Gulyas *et al.*, 1996), which is necessary for an efficient control of input plasticity of principal cells (Miles *et al.*, 1996). Electron microscopic examination revealed the structural basis of their potential role in the local circuit. The fate of calretinin-containing cells was studied in models of epilepsy and in human epileptic patients. However, there is a contradiction in the literature. In most cases a loss of calretinin-positive cells was found in animal models (Magloczky and Freund, 1993, 1995; Andre *et al.*, 2001; Slezia *et al.*, 2004; van Vliet *et al.*, 2004; Tang *et al.*, 2006). Reduction of their number was shown in the dentate gyrus of patients with epilepsy (Magloczky *et al.*, 2000). However, the preservation or even an increase of the number of calretinin-positive cells was observed by

Blumcke *et al.* (1996) in patients with human temporal lobe epilepsy.

To solve this contradiction we carried out detailed quantitative analyses of the number of calretinin-positive cells in all subfields of the hippocampus. Control hippocampi with different post-mortem delays were examined to reveal whether the resulting differences in preservation can influence the density of calretinin-positive cells. They were compared with surgically removed human epileptic hippocampi. In addition, the morphology of cells and synaptic target distribution of calretinin-positive terminals were examined to investigate the degree of synaptic reorganization of calretinin-containing cells in the CA1 region. We chose the CA1 region for further analyses to establish whether changes in target distribution of calretinin-positive axon terminals are associated with the severity of principal cell death.

Materials and methods

Hippocampal samples were obtained from patients with therapy-resistant temporal lobe epilepsy (*n* = 44) (Table 1). The seizure focus was identified by multimodal studies including video-EEG monitoring, MRI, single photon emission computed tomography and/or positron emission tomography. Patients with intractable temporal lobe epilepsy underwent surgery in the National Institute of Neuroscience in Budapest, Hungary within the framework of the Hungarian Epilepsy Surgery Program. A written informed consent for the study was obtained from every patient before surgery. Standard anterior temporal lobectomies were performed (Spencer and Spencer, 1985); the anterior third of the temporal lobe was removed together with the temporomedial structures.

Control hippocampi (*n* = 8, age 51–74 years) were kindly provided by the Lenhossek Human Brain Programme, Semmelweis Medical University, Budapest, Hungary. Control subjects died suddenly from causes unrelated to any brain disease and were processed for autopsies in the Department of Forensic Medicine of the Semmelweis University Medical School, Budapest, Hungary. Examination of medical records of control subjects at the autopsy confirmed the absence of any neurological disorders. Brains were removed 2–10 h after death.

The study was approved by the ethics committee at the Regional and Institutional Committee of Science and Research Ethics of Scientific Council of Health (TUKEB 5-1/1996, further extended in 2005) and performed in accordance with the Declaration of Helsinki.

After surgical removal, the epileptic tissue was immediately cut into 3–4 mm thick blocks and immersed into a fixative containing 4% paraformaldehyde, 0.1% glutaraldehyde and 0.2% picric acid in 0.1 M phosphate buffer (pH 7.4). Fixative was changed hourly to a fresh solution during constant agitation for 6 h, and the blocks were then post-fixed overnight, in the same fixative without glutaraldehyde. In the case of six samples (Controls 1, 6, 7, 9, 14 and 15) from the eight control hippocampi, the procedure was similar. To achieve better preservation for the quantitative analyses, two of the control brains (Controls 10 and 11) were removed from the skull after death (2 and 4 h, respectively), both internal carotid and vertebral arteries were cannulated and the brains were perfused first with physiological saline (2 l in 30 min) followed by a fixative solution containing 4% paraformaldehyde and 0.2% picric acid in 0.1 M phosphate buffer (6 l in 1.5 h). The hippocampus was removed after perfusion, cut into 3–4 mm thick blocks and post-fixed in the same fixative solution.

Table 1 Characteristics of the epileptic subjects

Pathological group	Patient's code number	Gender	Age (years)	Age at onset of epilepsy (years)	Duration of epilepsy (years)
1 (mild)	40	M	20	6	14
	54	F	22	15	7
	67	F	23	17	6
	79	M	47	8	39
	134	F	39	25	14
	138	F	50	19	31
2 (patchy)	15	M	25	8	17
	16	M	23	16	7
	30	F	40	1	39
	31	F	23	2	21
	38	F	23	10	13
	41	M	16	2	14
	42	F	43	13	30
	46	F	37	37	2 months
	47	F	30	15	15
	49	M	63	59	4
	59	M	32	7	25
	61	M	41	16	25
	68	M	44	20	24
	72	M	31	29	2
	73	F	27	10	17
	109	M	32	11 months	32
3 (sclerotic)	3	F	22	8 months	21
	4	M	31	24	7
	11	M	36	30	6
	18	M	32	20	12
	19	M	56	24	32
	21	M	30	21	9
	22	F	27	22	5
	29	F	29	5	24
	35	M	25	12	13
	36	F	45	31	14
	37	M	41	2	39
	53	M	26	17	9
	60	M	30	6	24
	62	F	45	25	20
	71	M	35	19	16
	74	M	34	8	26
	75	M	24	0.3	24
	83	F	29	6	23
	86	M	41	10	31
	90	F	46	11	35
	91	F	35	20	15
	92	F	35	5	30

Immunocytochemistry

Sixty micrometre thick Vibratome sections were cut from the blocks and sections were processed for immunostaining. Following washing in 0.1 M phosphate buffer (6 × 20 min), the sections were immersed in 30% sucrose in 0.1 M phosphate buffer for 1–2 days, then freeze-thawed three times over liquid nitrogen and washed in Tris-buffered saline (pH 7.4, 2 × 10 min). Endogenous peroxidase activity was blocked by 1% H_2O_2 in the first Tris-buffered saline for 10 min. Tris-buffered saline was used for all washes (3 × 10 min between each serum) and for dilution of the antiserum. Non-specific immunoglobulin binding of the tissue was blocked by 5% milk powder and 2% bovine serum albumin in Tris-buffered saline. A monoclonal mouse antibody against calretinin (1:5000, SWANT, Bellinzona, Switzerland) was used for 2 days at 4°C. The specificity of the antiserum was thoroughly tested by the laboratory of origin. For the visualization of immunopositive elements, biotinylated anti-mouse immunoglobulin G (1:250, Vector) was applied as secondary serum (2 h), followed by avidin-biotinylated horseradish peroxidase complex (1:250, Vector, 1.5 h). The sections were preincubated for 20 min in 3,3′-diaminobenzidine-tetrahydrochloride chromogen (DAB, 0.05 M, dissolved in Tris buffer pH 7.6) and then developed by 0.01% H_2O_2. Sections were then treated with 1% OsO_4 in phosphate buffer for 40 min, dehydrated in ethanol (1% uranyl acetate was added at the 70% ethanol stage for 40 min) and mounted in Durcupan (ACM, Fluka). The control hippocampi were processed in the same way. All samples (n = 44) were examined at the light microscopic level and classified according to their general pathological features. Hippocampi with gross lesion or severe tumour infiltration were not involved in this study. Representative patients showing the characteristic changes (three with mild or moderate and three with strong sclerosis) were chosen for further electron microscopic analysis. Layers of the CA1 region were re-embedded and sectioned for electron microscopy. Ultrathin serial sections were collected on Formvar-coated single slot grids, stained with lead citrate and examined in a Hitachi 7100 electron microscope.

Double immunostaining for calretinin/calbindin

The protocol was similar to that described above for single immunostaining. After blocking the endogenous peroxidase activity by 1% H_2O_2 and the non-specific immunoglobulin binding of the tissue by 10% normal horse serum (Vector, 40 min), the sections were first incubated in the antiserum against calretinin (1:5000, SWANT, Bellinzona, Switzerland) for 2 days. This was followed by biotinylated anti-mouse immunoglobulin G (1:250, 2 h, Vector) and then Elite avidin-biotinylated horseradish peroxidase complex (1:300, 1.5 h, Vector). In this case, calretinin was developed using DAB as a chromogen intensified with ammonium nickel-sulphate (DAB–Ni, black reaction product). After the first immunostaining the sections were washed extensively in Tris-buffered saline and the non-specific immunoglobulin binding of the tissue was blocked by 10% normal goat serum (Vector, 20 min). The sections were then incubated in a polyclonal rabbit antiserum against calbindin (1:1000, Baimbridge and Miller, 1982) for 2 days. After the incubation in the biotinylated anti-rabbit immunoglobulin G (1:250, 2 h, Vector) and avidin-biotinylated horseradish peroxidase complex (1:250, 1.5 h, Vector) this second immunoperoxidase reaction was developed with DAB as a chromogen (brown reaction product). Sections were then dehydrated in ethanol (without treatment with OsO_4 and uranyl acetate) and embedded in Durcupan (ACM, Fluka). The immunopositive profiles at the light microscopic level were identified by their colour difference (i.e. calretinin-positive profiles were black; the calbindin-positives were brown).

Quantitative analysis of the number of calretinin-positive cells

To obtain data on changes of the number of calretinin-positive cells, three to four representative sections of the hippocampi were drawn by

camera lucida from control samples with different post-mortem delays (Controls 6, 7 and 10 with short ~2–4 h and Controls 1, 14 and 15 with long ~8–10 h post-mortem delay) and from patients of different pathological groups (Patients 47, 67, 72, 79, 109, 134 and 138 with mild or moderate sclerosis, Patients 22, 60, 83, 90 and 91 with strong sclerosis). The drawings were scaled down and scanned. The area of each region was measured by the NIH ImageJ (US National Institutes of Health, Bethesda, MD) program. In each control and epileptic sample, the cells were counted and the cell number was determined per unit area (mm^2) in a 60 μm thick section. CA1, CA3, stratum, granulosum, stratum moleculare and hilus were measured separately. Data for stratum granulosum and stratum moleculare were pooled, since in some of the epileptic samples the exact border of these layers was not clearly defined due to granule cell dispersion. In the case of the CA1 region, the cell number was determined per unit length (mm) of the subfield (because of the radial shrinkage of the sclerotic CA1). The length was measured in the centreline of the CA1 region, which derived from the bisection of the distance between the alveus and stratum lacunosum-moleculare along the subfield. We determined the changes in the density of the presumable persisting calretinin-positive Cajal–Retzius cells as well in the outer molecular layer of dentate gyrus/hippocampal fissure. Cell number was determined per unit length (mm) of the molecular layer at the outer border. Since there was no significant difference between the epileptic samples with mild or moderate sclerosis (Types I and II, respectively), they were pooled and referred to as non-sclerotic tissues. Data were evaluated by the Statistica 6.0 program. Mann–Whitney *U*-test was applied.

Quantitative electron microscopic analysis

The post-synaptic target elements of calretinin-positive axon terminals were examined in two perfusion fixed control samples (Controls 10 and 11) and in epileptic samples (Patients 54, 79, 38 with mild or moderate sclerosis, Patients 21, 71, 75 with strong sclerosis). Strata oriens, pyramidale, radiatum and lacunosum-moleculare were re-embedded from the CA1 region and sectioned for electron microscopy. In the sclerotic cases, the separation of strata oriens, pyramidale and radiatum was not possible, therefore they were pooled. Serial sections were made from the blocks and calretinin-containing terminals were analysed in every 10th section in order, following the rules of systematic random sampling, to avoid sampling of the same axon terminals. Photographs were taken of every calretinin-positive synaptic terminal in each section, and the distribution of the post-synaptic target elements of the calretinin-immunoreactive terminals was determined. There was no significant difference between the epileptic samples with mild and moderate sclerosis (Type 1 and 2, respectively), therefore they were pooled and referred to as non-sclerotic samples.

Results

Dependence of calretinin-immunostaining on age, fixation and post-mortem delay

In a preliminary experiment we examined 12 control brains of different ages, from both genders, with different post-mortem delay. We found that age did not affect the quality and quantity of immunostaining if no central nervous system disorders had been diagnosed.

The preservation of the post-mortem perfused controls (Controls 10 and 11) and the immersion-fixed controls with short post-mortem delay was comparable to the immediately fixed epileptic samples and perfusion fixed animal tissues. In the control subjects, perfusion fixation resulted in better ultrastructural preservation than immersion fixation, therefore hippocampi removed from two perfusion-fixed brains were used for the electron microscopy quantitative analysis.

In a previous study, it was claimed that calretinin-immunostaining was sensitive to post-mortem delay (Urban *et al.*, 2002). Sensitivity of calretinin-containing interneurons in ischaemia was also demonstrated (Freund and Magloczky, 1993). On the other hand, in a study that used control samples with long post-mortem delays, calretinin-positive neurons were shown to be resistant in epilepsy (Blumcke *et al.*, 1996).

In the present study, we examined quantitatively the effect of post-mortem delay on the number and distribution of calretinin-positive elements and the control samples, with different post-mortem delays, were compared to the epileptic samples. The changes in the density, morphology and post-synaptic target specificity of the calretinin-immunoreactive neurons were examined in 17 epileptic and 8 control human hippocampi. The general qualitative description of the morphology and distribution of the calretinin-positive cells was based on a careful analysis of all samples included in the study (44 epileptic and 8 control samples).

Pathological classification of the epileptic samples

All patients examined in the present study had therapy resistant epilepsy of temporal lobe origin (Table 1). The patients had different degrees of hippocampal atrophy and/or sclerosis. All the examined sections were derived from the anterior part of the hippocampal body. Similarly to our previous studies (Wittner *et al.*, 2002, 2005; Toth *et al.*, 2007) and recent results (de Lanerolle *et al.*, 2003), patients with epilepsy were classified on the basis of principal cell loss and interneuronal changes examined at the light microscopic level as follows.

(i) Epileptic Type 1 (mild) (*n* = 6): similar to control, no considerable cell loss in the CA1 region, pyramidal cells present, layers are visible and intact, their borders are clearly identified. There is a slight loss in certain interneuron types, mostly in the hilus and the stratum oriens of the CA1 region.

(ii) Epileptic Type 2 (patchy) (*n* = 16): pyramidal cell loss in patches in the CA1 pyramidal cell layer but these segments of the CA1 region are not atrophic. Interneuron loss is more pronounced.

(iii) Epileptic Type 3 (sclerotic) (*n* = 22): the CA1 region is shrunken, atrophic, more than 90% of principal cells are missing and occasionally scattered pyramidal cells remain in the CA1 region. Only the stratum lacunosum-moleculare is present as a distinct layer in the CA1 region, the others could not be separated from each other due to the lack of pyramidal cells and their dendrites and the shrinkage of the

tissue. This remaining part should contain the layers identified in the control as stratum oriens, stratum pyramidale and stratum radiatum. Mossy fibre sprouting and considerable changes in the distribution and morphology of interneurons can be observed in the samples of this group.

The number, morphology and distribution of cells were similar in patients in the same pathological group, but differed between the groups. The control samples with short (2–4 h) post-mortem delay were similar to each other and differed from the epileptic groups. Therefore, we concluded that the differences found between control and epileptic tissues in the present study are likely to be caused by epilepsy.

Number and distribution of calretinin-immunostained cells in the human hippocampus

We have examined the number and distribution of calretinin-immunoreactive cells in control samples with different post-mortem delays (Fig. 1) and in the hippocampi of patients with epilepsy with varying degrees of principal cell death (Fig. 2).

In control samples with short post-mortem delay (2–4 h), calretinin-containing cells were present in all regions of the hippocampus. Numerous cells were immunopositive in the hilus of the dentate gyrus (Fig. 1A) and in the stratum pyramidale and radiatum of CA1 (Fig. 1C), especially at the border of stratum lacunosum-moleculare. Cell numbers were low in the stratum granulosum and moleculare of the dentate gyrus (Fig. 1A) and in the stratum oriens and lacunosum-moleculare of the CA1 (Fig. 1C). The CA2 and CA3 regions contained only a few immunopositive cells (Urban *et al.*, 2002) (Table 2, Fig. 3).

Although the general distribution was similar, a significantly smaller number of calretinin-immunostained cells was present in every subregion of control samples with long post-mortem delay (Table 2, Fig. 1B and D, and 3) (strata granulosum and moleculare: 34.3%, hilus: 43.9%, CA1: 23.5%, CA3: 28% of control samples with short post-mortem delay).

In the non-sclerotic epileptic tissues, the calretinin-positive cell number was similar to the control samples with short post-mortem delay (Fig. 2A–C), only the CA3 region and the hilus showed a significant reduction in the immunolabelled cell number (Table 2, Fig. 3) (strata granulosum and moleculare: 74.9%, hilus: 65.4%, CA1: 66.7%, CA3: 60.5% of control samples with short post-mortem delay). In contrast, in the non-sclerotic samples, considerably more immunopositive cells could be seen in each subregion than in control samples with long post-mortem delay (Table 2, Fig. 3).

The number of calretinin-immunoreactive cells was significantly decreased in CA3, hilus and strata moleculare and granulosum of the dentate gyrus of the sclerotic epileptic cases compared to the control samples with short post-mortem delay (Table 2, Figs 2A and D, and 3) (strata granulosum and moleculare: 35.2%, hilus: 32.1%, CA1: 76.1%, CA3: 21.9% of control samples with short post-mortem delay).

The CA1 region displayed a significant shrinkage in the sclerotic hippocampi, which may explain why there was no difference in the number of cells per area in this region. Determining the cell number per unit length of the CA1 region (mm), there was a significant difference in this subfield (Table 2, Fig. 3) (34.1% of control samples with short post-mortem delay).

In addition, the number of presumed Cajal–Retzius cells at the border of the stratum moleculare-hippocampal fissure was calculated separately, since in a previous study their number was found to be larger than in controls (Blumcke *et al.*, 1999; Thom *et al.*, 2002). We found that their number was significantly decreased in the control samples with long post-mortem delay as well as in the sclerotic tissues and even in the non-sclerotic cases (Table 2, Fig. 3) (24.8, 46.4 and 56.8% of control samples with short post-mortem delay, respectively).

Morphology of calretinin-immunoreactive cells

The morphology of the calretinin-positive neurons in the control human hippocampus has been described by Nitsch and Ohm (1995). They formed a heterogeneous cell population with large, multipolar cells in the hilus, spindle shaped cells in the strata moleculare and oriens, a population of small cells in the entire dentate gyrus and multipolar cells, scattered through the layers of the CA1-3 (Fig. 1A and C).

Calretinin-positive cells usually had few dendrites, these were typically smooth, occasionally spiny. In the CA1 region long, smooth, radially oriented dendrites could be seen which were often juxtaposed and ran parallel, in close contact (Fig. 1E and F). In these juxtaposed segments, puncta adherentia could be observed in high-power electron micrographs (Urban *et al.*, 2002). Based on their connectivity, they appeared to participate in dendritic and interneuron-specific inhibition (Urban *et al.*, 2002).

Besides the reduction in number, the morphology of the calretinin-positive cells was also altered in the control samples with long post-mortem delay. The few remaining calretinin-containing cells had no or 1–2 strongly varicose, short, degenerating dendrites (Fig. 1G).

In epileptic cases, the calretinin-positive cells were preserved in the non-sclerotic samples but their morphology showed considerable alteration. The extension and orientation of the dendritic trees were similar to that seen in control tissues but the dendrites were varicose, segmented and showed signs of degeneration. The enlarged beads were connected by thin segments or were entirely separated (Fig. 2E). Contacts between calretinin-positive dendrites originating from different calretinin-containing cells were less frequently seen.

In sclerotic cases, most of the surviving calretinin-positive cells lost their dendritic tree or had 1 or 2 considerably shorter and segmented dendrites. The complete separation of the dendritic varicosities was also often observed (Fig. 2F). In the sclerotic CA1 region most of the remaining calretinin-positive dendrites had a horizontal orientation.
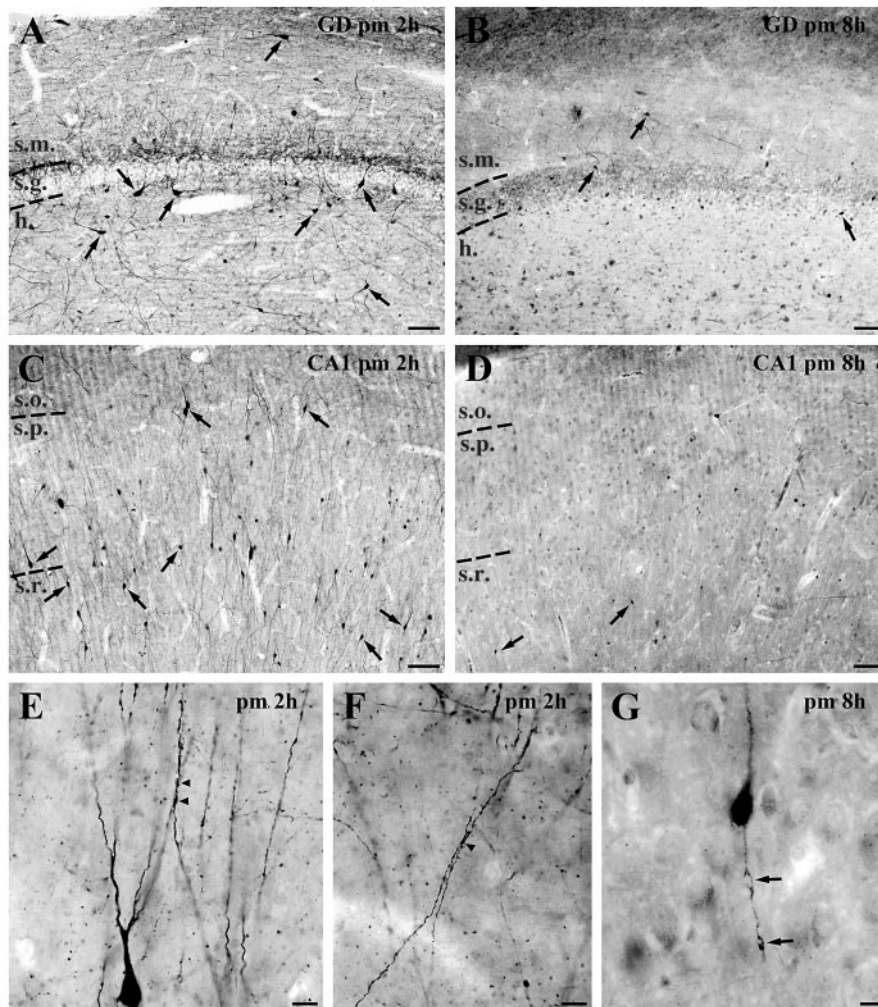
Figure 1 Distribution and morphology of calretinin-positive cells in the human control hippocampus. (**A**) Dentate gyrus (GD), 2 h post-mortem (pm). Large cells in the hilus, horizontal cells in the molecular layer, as well as the small cells that are present in every layer are characteristic of well preserved control samples with short post-mortem delay. (**B**) Dentate gyrus, 8 h post-mortem. The majority of calretinin-immunoreactive cells disappear from the dentate gyrus. (**C**) CA1 region, 2 h post-mortem. Numerous immunoreactive cells with smooth dendrites can be seen in all layers of the CA1 subfield in control samples with short post-mortem delay. The mainly radially oriented cells are most frequent in the strata pyramidale (s.p.) and radiatum (s.r.). (**D**) CA1 region, 8 h post-mortem. In these samples hardly any calretinin-positive cells can be found in the CA1 region, and even those have a degenerating dendritic tree. (**E**, **F** and **G**) High-power light micrographs show the morphology of the calretinin-positive dendrites in the control CA1 region. Long, vertically oriented dendrites which are often juxtaposed and run together over short segments can be seen in control samples with short post-mortem delay (arrowheads, **E** and **F**). In control samples with long post-mortem delay, the dendrites show signs of degeneration, the enlarged beads are connected by thin segments (**G**). Scale bars: **A–D** = 100 μm; **E–G** = 20 μm; s.m. = stratum moleculare; s.g. = stratum granulosum; h = hilus; s.o. = stratum oriens.

Electron microscopic features of calretinin-immunoreactive profiles

Electron microscopy studies were carried out to reveal whether the synaptic target specificities of calretinin-positive inter-neurons changed in the epileptic tissues. Two perfusion fixed controls and six epileptic samples were examined (three non-sclerotic and three with severe sclerosis). We chose to study the CA1 region to investigate whether reorganization of calretinin-positive axon terminals was associated with the severity of principal cell death.

The general ultrastructural features of calretinin-positive cells in the control CA1 region were similar to those described previously in monkey and human samples (Seress *et al*., 1993*b*; Nitsch and Ohm, 1995; Urban *et al*., 2002). The cytoplasmic rim surrounding the nucleus was usually thin and contained a moderate number of mitochondria. The majority of the synaptic inputs were confined to the dendrites of calretinin-positive cells. Terminals targeting the somata were only occasionally seen ($n = 2$ out of 23 cell bodies, examined in single sections). Puncta or zona adherentia-type contacts were often observed between juxtaposed calretinin-positive dendrites.
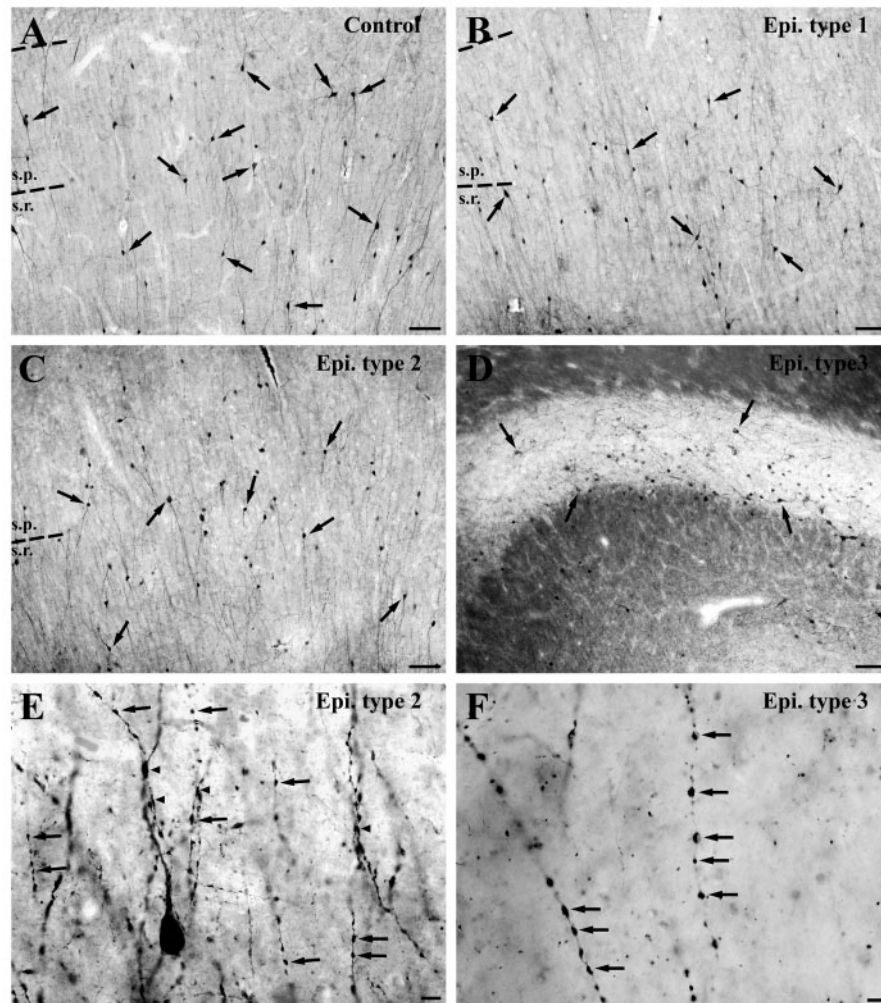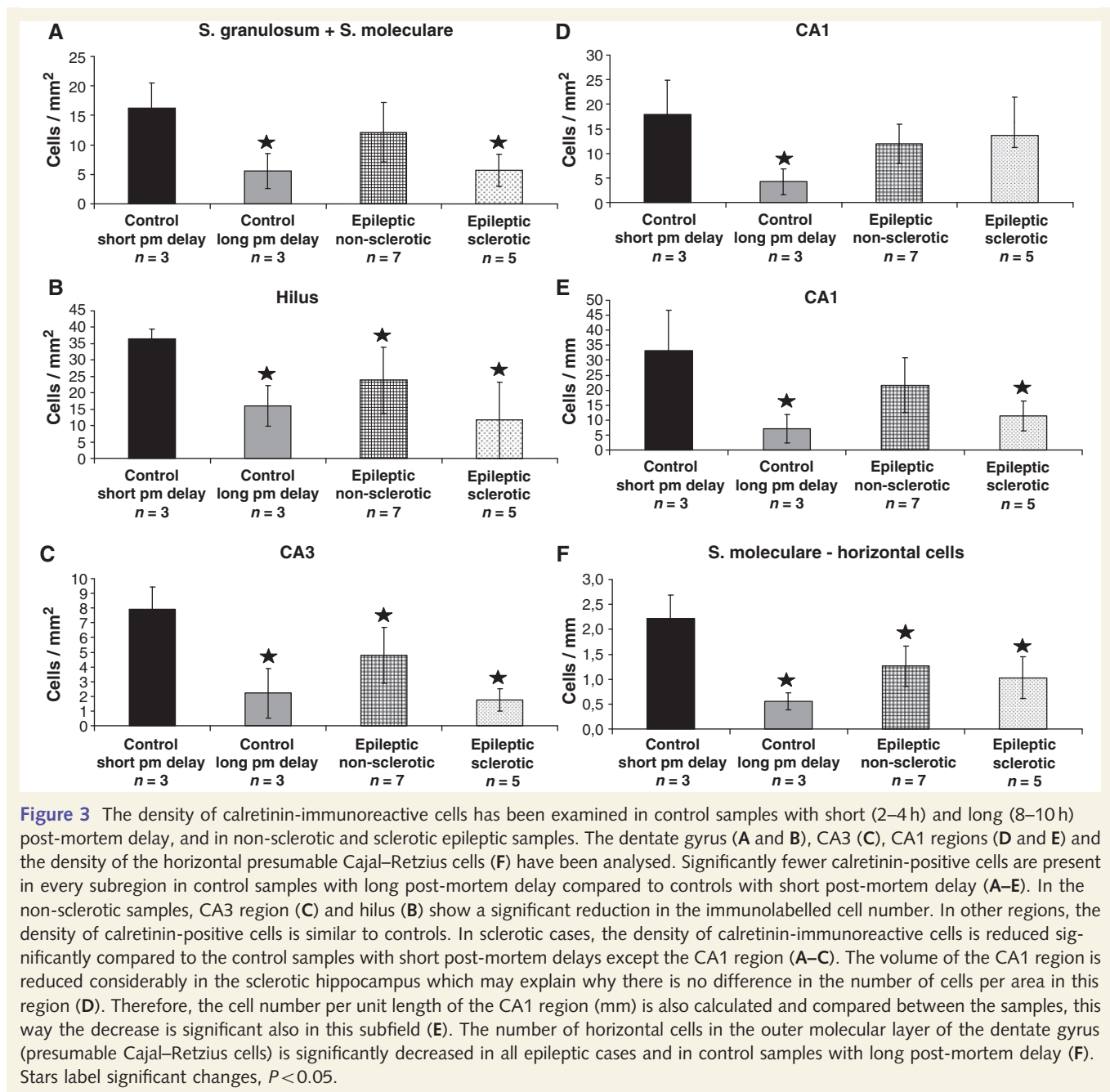
Figure 2 Distribution and morphology of calretinin-positive cells in the human control and epileptic CA1 region. (**A**) Numerous immunoreactive cells with smooth dendrites can be seen in all layers of the CA1 region in control samples with short post-mortem delay. (**B** and **C**) The number of immunolabelled cells and the extent of their dendritic trees are quite similar in the non-sclerotic Type 1 (**B**) and Type 2 (**C**) samples compared to controls, although in the latter cases the dendrites are varicose and segmented. (**D**) The number of calretinin-positive cells is decreased significantly in the sclerotic epileptic cases. The area of the sclerotic hippocampi is reduced because of the shrinkage of the CA1 region caused by the loss of CA1 pyramidal cells. (**E** and **F**) High-power light micrographs show the morphological alterations of the calretinin-positive dendrites in epileptic cases. In the non-sclerotic Type 2 samples (**E**), almost all of them show signs of degeneration, the dendrites have become beaded and segmented (arrows, **E**). Dendro-dendritic connections are less frequent than in controls (arrowheads, **E**). In sclerotic cases (**F**) only fragmented dendrites can be seen, most of the beads are separated (arrows, **F**). Scale bars: **A–D** = 100 μm; **E** and **F** = 20 μm; s.p. = stratum pyramidale; s.r. = stratum radiatum.

Table 2 Data of the density of calretinin-positive cells

	Mean ± standard deviation			
	Control short post-mortem delay (2–4 h) $n=3$	Control long post-mortem delay (8–10 h) $n=3$	Epileptic non-sclerotic $n=7$	Epileptic sclerotic $n=5$
Granulosum and moleculare (cells/mm^2)	16.2 ± 4.3	5.6 ± 3.0	12.1 ± 5.0	5.7 ± 2.7
Hilus (cells/mm^2)	36.5 ± 3.1	16.0 ± 6.1	23.8 ± 10.1	11.7 ± 11.6
CA3 (cells/mm^2)	7.9 ± 1.5	2.2 ± 1.7	4.8 ± 1.9	1.7 ± 0.8
CA1 (cells/mm^2)	17.9 ± 7.0	4.2 ± 2.6	11.9 ± 3.9	13.6 ± 5.1
CA1 (cells/mm)	33.2 ± 13.5	7.1 ± 4.7	21.7 ± 9.1	11.3 ± 5.0
Horizontal cells at the border of stratum moleculare-lacunosum-moleculare (cell/mm)	2.2 ± 0.5	0.6 ± 0.2	1.3 ± 0.4	1.0 ± 0.4

Figure 3 The density of calretinin-immunoreactive cells has been examined in control samples with short (2–4 h) and long (8–10 h) post-mortem delay, and in non-sclerotic and sclerotic epileptic samples. The dentate gyrus (**A** and **B**), CA3 (**C**), CA1 regions (**D** and **E**) and the density of the horizontal presumable Cajal–Retzius cells (**F**) have been analysed. Significantly fewer calretinin-positive cells are present in every subregion in control samples with long post-mortem delay compared to controls with short post-mortem delay (**A–E**). In the non-sclerotic samples, CA3 region (**C**) and hilus (**B**) show a significant reduction in the immunolabelled cell number. In other regions, the density of calretinin-positive cells is similar to controls. In sclerotic cases, the density of calretinin-immunoreactive cells is reduced significantly compared to the control samples with short post-mortem delays except the CA1 region (**A–C**). The volume of the CA1 region is reduced considerably in the sclerotic hippocampus which may explain why there is no difference in the number of cells per area in this region (**D**). Therefore, the cell number per unit length of the CA1 region (mm) is also calculated and compared between the samples, this way the decrease is significant also in this subfield (**E**). The number of horizontal cells in the outer molecular layer of the dentate gyrus (presumable Cajal–Retzius cells) is significantly decreased in all epileptic cases and in control samples with long post-mortem delay (**F**). Stars label significant changes, $P < 0.05$.

In the non-sclerotic epileptic samples, most of the calretinin-immunolabelled cell bodies were similar to the controls. However, in the sclerotic tissues, several degenerating calretinin-positive cell bodies were seen with strongly infolded or partially segmented nucleus. Total fragmentation of the cell content was also observed.

The ultrastructure of varicose and segmented dendrites of the epileptic CA1 region was analysed with the electron microscopy (Fig. 4B). The dendritic structure showed signs of degeneration even in the non-sclerotic samples. Distorted mitochondria and degrading cytoplasmic matrix were characteristic of the varicose swellings (Fig. 4B). Puncta or zona adherentia-like contacts between calretinin-positive dendritic shafts were rarely seen both in the sclerotic and non-sclerotic epileptic cases.

In the epileptic samples, the mass of the glial elements was increased compared to the controls. The calretinin-positive dendritic shafts were often covered with glial processes (Figs 4B and 5).

Post-synaptic target distribution of calretinin-positive axon terminals at the electron microscopy level

Two types of calretinin-positive synaptic terminals were found. One of them formed symmetric synaptic contacts and was found in all layers of the CA1 region. The other type established asymmetric contacts and was confined to stratum
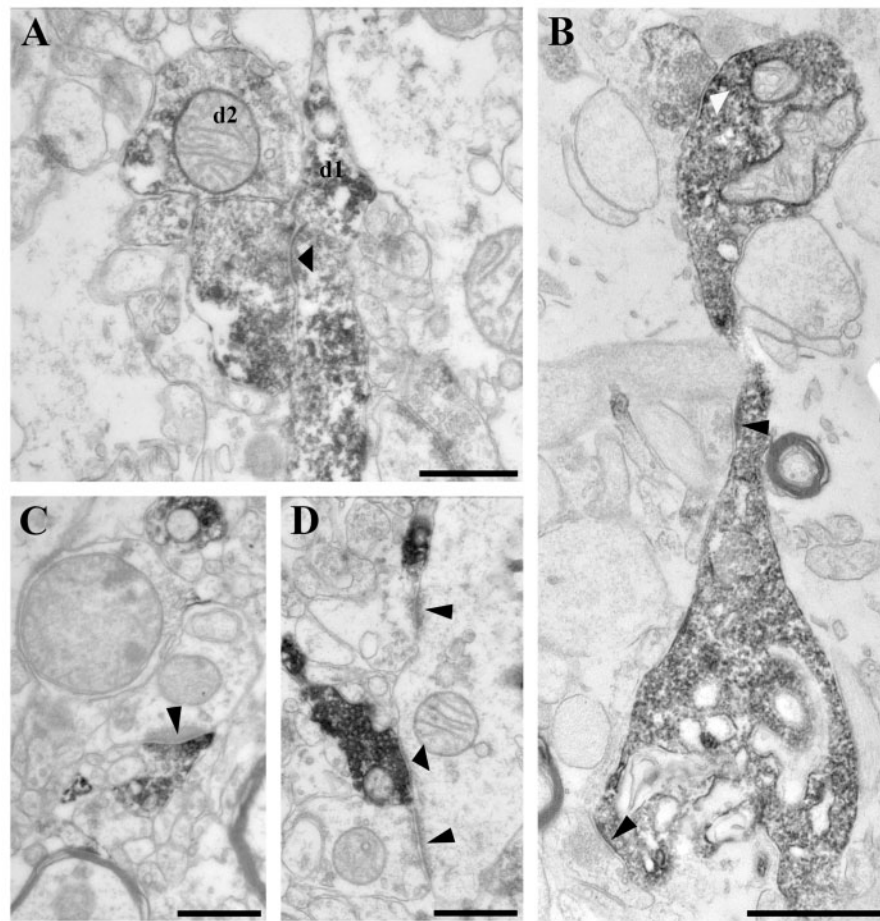
Figure 4 High-power electron micrographs from control (**A**, **C** and **D**) and epileptic (**B**) CA1 region. Terminals of calretinin-positive interneurons establish symmetric synaptic contacts (**A**, **B** and **D**, thick arrowheads). They frequently terminate on other calretinin-positive interneuron dendrites (**A**; d1). Dendrites of unlabelled interneurons also receive synaptic contacts from calretinin-positive inhibitory terminals (**D**). At the border of stratum lacunosum-moleculare a part of the calretinin-positive terminals establish asymmetric synaptic contacts with very thick post-synaptic density most frequently targeting unlabelled dendrites (**C**, thin arrowheads). **B** shows a varicose dendrite surrounded by glial processes. The beads are degenerating, although they still receive synaptic input, a symmetric synaptic contact from a calretinin-immunopositive bouton (thick white arrowhead) and two asymmetric synaptic contacts from unlabelled terminals (thin black arrowheads). Scale bars: **A**, **C** and **D** = 0.5 µm; **B** = 10 µm.

lacunosum-moleculare (Urban *et al*., 2002). The former were the axon terminals of local calretinin-containing interneurons whereas the latter presumably originated from the thalamic nucleus reuniens (Amaral and Cowan, 1980; Bokor *et al*., 2002). The symmetric and asymmetric contacts were clearly distinguishable based on the thickness of the post-synaptic density.

In controls, the majority of calretinin-positive terminals established symmetric synapses in the stratum oriens and pyramidale (100%, $n = 54$ and 98%, $n = 83$, respectively) (Fig. 4A and D), whereas in the stratum lacunosum-moleculare almost half (44%, $n = 98$) established asymmetric synapses mainly with unstained dendrites and spines (Fig. 4C). The relative ratios of calretinin-containing terminals giving asymmetric synapses increased and those giving symmetric synapses decreased in the human epileptic CA1 region (Fig. 5C, E and F). The ratio of the symmetric synapses decreased in strata oriens and lacunosum-moleculare (84%, $n = 81$

and 20%, $n = 175$, respectively) and in the oriens-pyramidale-radiatum of the sclerotic samples (66%, $n = 91$).

In the present study, we focused on the target distribution of local calretinin-containing interneurons giving symmetric synaptic contacts.

The post-synaptic elements were classified according to their electron microscopy morphology or calretinin content, as pyramidal cell dendrites, unstained interneuron dendrites, calretinin-positive interneuron dendrites and spines, as well as unidentified dendrites. The identification was based on the location and morphology of dendrites and synaptic input of the given dendritic shaft. Interneuron dendrites usually have larger mitochondria with characteristic morphology and pyramidal dendritic shafts receive no asymmetric synapses in the rat (Megias *et al*., 2001).

In control samples, the most frequent post-synaptic targets of calretinin-positive cells were calretinin-positive dendrites (23%)
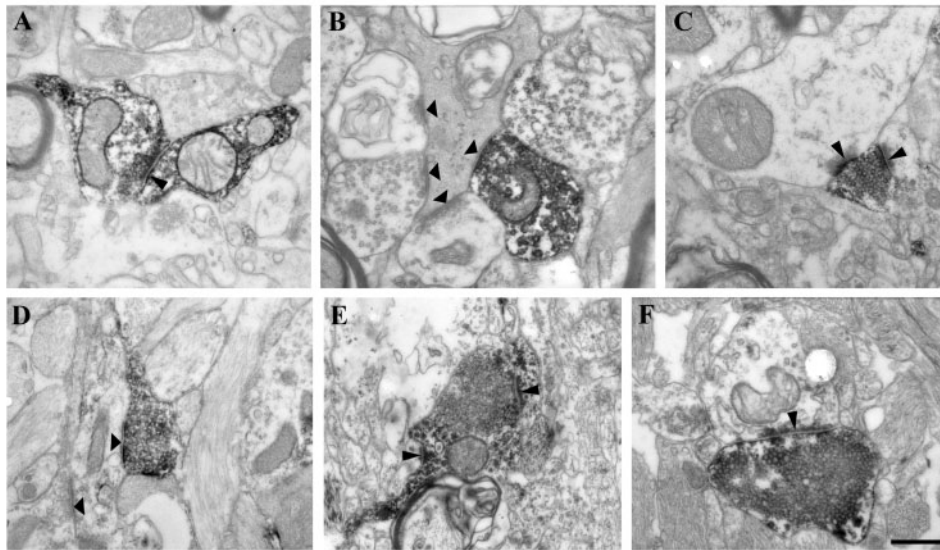
Figure 5 High-power electron micrographs from epileptic non-sclerotic (**A**, **B** and **C**) and sclerotic (**D**, **E** and **F**) CA1 region. Calretinin-positive terminals establishing symmetric synaptic contacts on calretinin-immunostained dendrites are less frequent in the epileptic tissues (**A**, thin arrowhead). They mainly target unlabelled interneuron dendrites both in non-sclerotic and sclerotic cases (**B** and **D**, thick arrowheads). (**B**) A degenerating interneuron dendrite still receives several symmetric synaptic contacts, one from a calretinin-positive and three from unlabelled interneurons (thick arrowheads). (**C**) A calretinin-positive terminal from the stratum lacunosum-moleculare establishes asymmetric synaptic contacts on an unstained interneuron dendrite and on a spine (thin arrowheads). In sclerotic tissues, the most frequent targets of calretinin-positive interneurons are also unlabelled interneuron dendrites (**D**, thick arrowheads). The ratio of calretinin-positive terminals give asymmetric synaptic contacts is increased in epilepsy. (**E** and **F**) Calretinin-positive terminals give asymmetric synaptic contacts on a calretinin-positive dendrite, on a spine (**E**) and on an unstained interneuron dendrite (**F**). Scale bar = 0.5 μm.

(Figs 4A and 6) and pyramidal cell dendrites (22.4%) (Fig. 6). Unlabelled interneuron dendrites (Figs 4D and 6) and spines were less frequently observed among the targets (7.6 and 2.12%, respectively). The remaining 44.8% of the targets could not be unequivocally identified. However, in epileptic tissues there were significantly fewer calretinin-positive dendrites among the post-synaptic targets (5.13% in non-sclerotic and 3.16% in sclerotic cases) (Figs 5A and 6). In the non-sclerotic samples the most frequent targets were unlabelled interneuron dendrites (35.9%) (Figs 5B and 6). Pyramidal cell dendrites also occurred among the targets although in lower numbers than in controls (10.26%) (Fig. 6). Spines were rarely contacted (2.56%). In the sclerotic tissues the most frequent targets were also unstained interneuron dendrites (44.19%) (Figs 5D and 6). Pyramidal-like dendrites were not present among the targets partly due to the extensive pyramidal cell loss.

Identity of interneuronal targets of calretinin-positive terminals in the CA1 region

Calretinin-positive interneurons are known to be interneuron-selective inhibitory cells innervating mostly calbindin-positive interneurons in the CA1 region of the rat (Gulyas *et al.*, 1996). Previous studies have shown that in humans, a part of them also belong to this functional group of interneurons (Urban

et al., 2002). However, no evidence has shown that calretinin-containing cells indeed terminate on calbindin-containing interneurons in the human hippocampus.

To investigate whether calbindin-containing interneurons—that mainly terminate in the dendritic region of pyramidal cells and survive in large numbers in the epileptic hippocampus (Wittner *et al.*, 2002)—are among the targets of calretinin-immunopositive interneurons in humans, we performed calretinin–calbindin double-immunolabelling in control and epileptic samples using DAB/DAB–Ni method at the light microscopy level. The immunopositive profiles were identified by their colour difference (i.e. calretinin-positive profiles were black, calbindin-positives were brown).

Immunostaining was carried out for calbindin-labelled interneurons (brown reaction product) in all layers, as well as pyramidal cells in the control CA1. Calbindin-positive interneurons and pyramidal cells were clearly distinguishable, since interneurons had a stronger staining intensity (Seress *et al.*, 1991, 1992; Wittner *et al.*, 2002), a bipolar or multipolar morphology (Seress *et al.*, 1991) and were located in all layers (Freund and Buzsaki, 1996).

Immunostaining for calretinin-labelled interneurons (black reaction product) in the CA1 region as described above and an axonal cloud in all layers with the highest density in the inner third of the stratum moleculare and in the upper third of the stratum lacunosum-moleculare.

We found that the dendrites of calbindin-positive interneurons often received multiple contacts from calretinin-positive axon
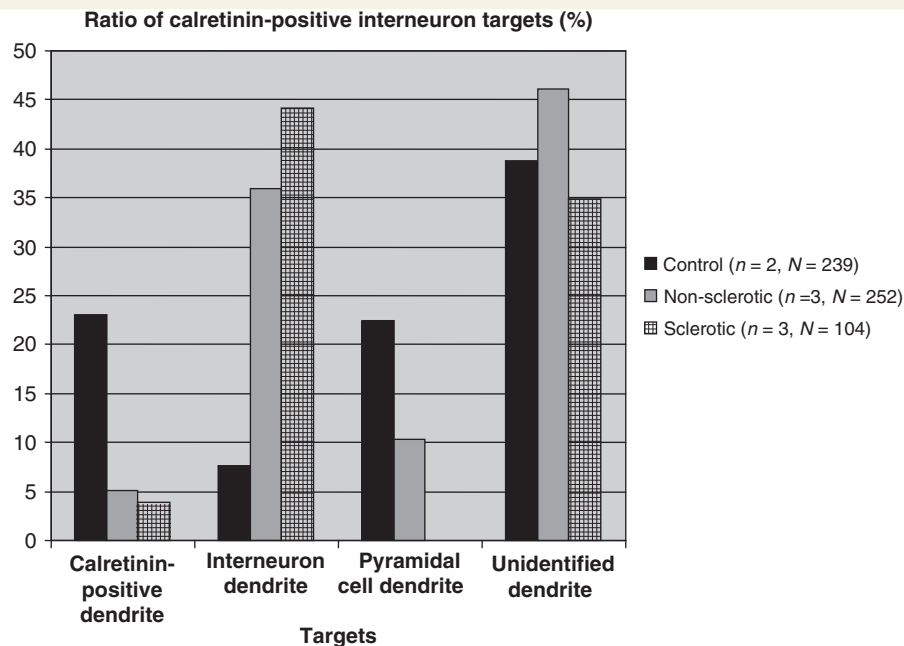
Figure 6 The target distribution of calretinin-positive interneurons is changed in the CA1 region of the epileptic human hippocampus. In controls, the calretinin-positive interneurons terminate on other interneuron dendrites (mainly on calretinin-positive and less frequently on unlabelled ones) and on principal cell dendrites. Ratio of calretinin-positive dendrites among the targets is decreased both in non-sclerotic and sclerotic samples. The ratio of terminals targeting unlabelled interneuron dendrites is increased in both groups. Ratio of pyramidal cell dendrites is decreased in non-sclerotic samples. In sclerotic cases pyramidal cell dendrites are not present among the targets. n = number of examined subjects; N = number of examined calretinin-positive axon terminals.

terminals both in control (Fig. 7A) and non-sclerotic epileptic samples (Fig. 7B). These were presumably inhibitory contacts originating from local calretinin-positive interneurons. The examined calbindin-positive dendritic segments were located in the stratum oriens or radiatum, close to the stratum pyramidale. A previous electron microscopy study proved that these layers were devoid of calretinin-positive terminals giving asymmetric synapses (Urban et al., 2002).

Discussion

Dependence of calretinin-immunostaining on age, fixation and post-mortem delay

The results revealed that the number of calretinin-immunostained cells is greatly influenced by the post-mortem delay. The best immunolabelling and the highest calretinin-positive cell number were obtained from the control samples with short post-mortem delay and perfusion fixation. In the control samples with long post-mortem delay, the number of immunopositive cells was significantly decreased (Figs 1 and 3). It was previously shown in a rat model that calretinin-containing interneurons were sensitive to ischaemia and became argyrophilic 6 h after ischaemia (Freund and Magloczky, 1993). Our results suggest that these inhibitory cells in humans are also sensitive to ischaemic conditions and long

post-mortem delay before fixation. Therefore, examination of changes of the density of calretinin-positive cells should be carried out only in comparison with carefully selected human samples with short post-mortem delays and high-quality fixation.

Impairment of calretinin-positive interneurons in epilepsy

Similarly to animal models (Freund and Magloczky, 1993; Magloczky and Freund, 1993; Andre et al., 2001; Slezia et al., 2004; Tang et al., 2006), calretinin-positive interneurons in humans are sensitive to epilepsy. Parallel with the degree of principal cell death, the number of calretinin-positive cells in epileptic human hippocampus was changed; they were preserved in the non-sclerotic cases, whereas their number was significantly decreased in the sclerotic samples (Figs 2 and 3). In the CA3 subfield and in the hilus, only a small number of cells survived even in the non-sclerotic hippocampi, therefore calretinin-positive cells in these regions have the highest susceptibility to epilepsy. The higher vulnerability of the calretinin-immunoreactive cells in the CA3 region and in the hilus might be explained by an enhanced input from sprouting mossy fibres (Shan et al., 2002).

These observations are in contradiction with an earlier study suggesting that human calretinin-positive neurons were resistant to epilepsy or even increased in number (Blumcke et al., 1996). These results may be explained by long post-mortem delays of control samples that, as shown in the present study, give rise to
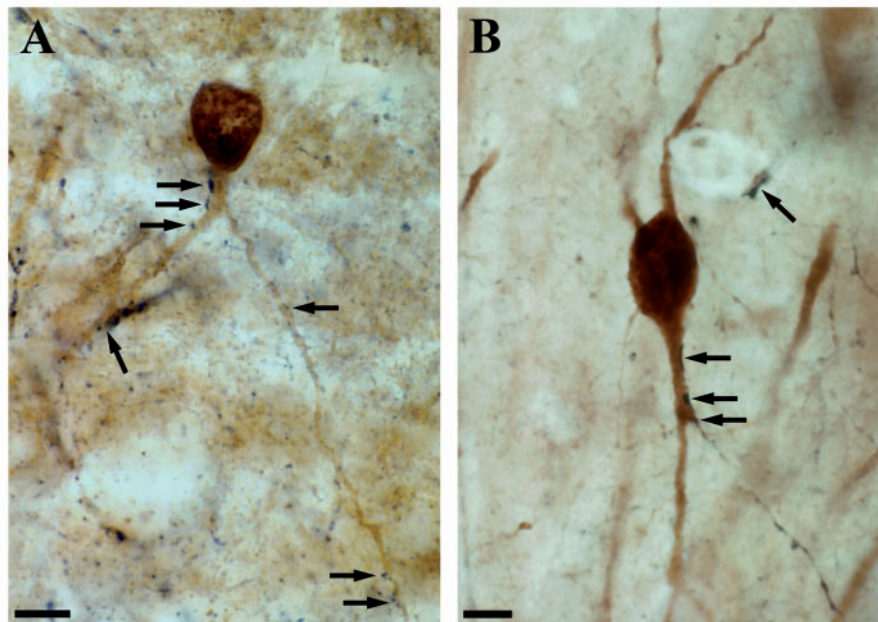
Figure 7 Double immunolabelling for calbindin and calretinin using DAB and DAB–Ni as chromogens. The control CA1 immunostaining for calbindin (DAB, brown reaction product) labels interneurons in all layers and pyramidal cells. Calbindin-positive interneurons and pyramidal cells are clearly distinguishable on the basis of the intensity of staining, their morphology and location. Immunostaining for calretinin (DAB–Ni, black reaction product) labels numerous interneurons in the CA1 region. The dendrites of calbindin-positive interneurons often receive multiple contacts from calretinin-positive axon terminals both in control (**A**, arrows) and non-sclerotic epileptic (**B**, arrows) samples. These are presumably inhibitory contacts originating from local calretinin-positive interneurons. The examined calbindin-positive dendritic segments are located in the stratum oriens or radiatum close to the stratum pyramidale, these layers are devoid of calretinin-positive terminals giving asymmetric synapses. Scale: 10 µm.

the disappearance of the majority of calretinin-immunoreactive cells. Horizontal calretinin-containing cells in the stratum molecu-lare near the hippocampal fissure were shown to be increased in number in epileptic samples (Blumcke *et al.*, 1999; Thom *et al.*, 2002) and referred to as Cajal–Retzius cells. Abraham and Meyer (2003) revealed that the majority of these calretinin-containing cells proved to be Cajal–Retzius cells expressing reelin. Reelin and Cajal–Retzius cells were shown to participate in epileptic net-works and activity since granule cell dispersion was prevented by addition of exogenous reelin in experimental epilepsy (Heinrich *et al.*, 2006; Muller *et al.*, 2009). Thus, it is important to clarify their fate in human epilepsy. In the present study, detailed quan-titative analyses of this area revealed that the number of calretinin-immunostained cells has also decreased in this region (Table 2, Fig. 3). Our results are consistent with studies showing that calretinin-positive interneurons are sensitive to epileptic activ-ity (Magloczky and Freund, 1993; Magloczky *et al.*, 2000; Suckling *et al.*, 2000; Andre *et al.*, 2001; Slezia *et al.*, 2004; van Vliet *et al.*, 2004; Tang *et al.*, 2006) and indicate that reelin-containing Cajal–Retzius cells are also vulnerable.

The question emerges whether calretinin-immunoreactive cells are indeed lost in the sclerotic cases, whether calretinin expression has decreased in the neurons or if antigen recognition is impaired due to an alteration of the protein conformation, e.g. in case of another calcium-binding protein, parvalbumin (Johansen *et al.*, 1990; Magloczky and Freund, 1995; Wittner *et al.*, 2001). The

latter two possibilities are unlikely because the degeneration of calretinin-containing cells was observed both at the light and elec-tron microscopy levels in the animal models of epilepsy (Magloczky and Freund, 1993; Andre *et al.*, 2001; Slezia *et al.*, 2004; Tang *et al.*, 2006) and ischaemia (Freund and Magloczky, 1993), as well as in human studies (Magloczky *et al.*, 2000; Suckling *et al.*, 2000), including the present study. Therefore the decreased number of calretinin-immunoreactive elements most likely reflects irreversible damage of these neurons.

The morphology of surviving calretinin-positive cells changed in the epileptic samples, the dendrites became beaded and seg-mented (Fig. 2). Electron microscopy examination revealed that the dendritic structure was damaged even in the non-sclerotic cases (Fig. 4B), where both calretinin-positive cells and principal cells were still present in large numbers. An explanation of the presence of varicose dendrites might be excitotoxic injury.

In controls, long segments of calretinin-positive dendrites origi-nating from different cells were often attached to each other and were connected by zona adherentia (Fig. 1) (Urban *et al.*, 2002). Zona adherentia can be observed between parvalbumin-immunostained dendrites in the control (Seress *et al.*, 1993*a*) and epileptic human hippocampi (Wittner *et al.*, 2005) as well as in the vicinity of gap junctions in rat (Kosaka and Hama, 1985), and they are thought to ensure the mechanical connection of dendrites that form dynamic gap junctions. Presence of these structures between calretinin-positive dendrites may result in an

electrically coupled, synchronized network of the connected cells. Zona adherentia were rarely observed in epileptic cases. The damage of dendrites—formation of large varicosities and even fragmentation—and the lack of zona adherentia may prevent the effective synchronization of dendritic inhibitory cells. Therefore we propose that functioning of calretinin-containing inhibitory cells may be impaired even before their number significantly decreases.

The target specificity of calretinin-positive interneurons is altered in the epileptic samples

The relative ratio of calretinin-positive terminals giving asymmetric synapses was found to be increased in the epileptic tissues. This might be explained by the decreased amount of calretinin-positive interneuronal boutons due to the degeneration in non-sclerotic cases and the extensive calretinin-containing cell loss in sclerotic cases. However, the sprouting of excitatory fibres with extrahippocampal (nucleus reuniens) origin can not be excluded, like in the case of the supramammillo hippocampal pathway (Magloczky et al., 2000).

The target specificity of calretinin-positive interneurons has changed in the CA1 region of the epileptic human hippocampus. In control samples, the most frequent post-synaptic targets of calretinin-positive interneurons were calretinin-positive dendrites, pyramidal cell dendrites and unlabelled interneuron dendrites. However, in epileptic tissues there were significantly fewer calretinin-positive dendrites and pyramidal cell dendrites among the post-synaptic targets (Fig. 6).

These results suggest that the synaptic reorganization of the hippocampal network involving calretinin-containing interneurons has already started without any significant pyramidal- and calretinin-containing cell death in the CA1 region. The fact that the ratio of post-synaptic pyramidal cell dendrites has been decreased in non-sclerotic cases may reflect the higher vulnerability of calretinin-positive interneurons targeting the dendritic region of principal cells. A decreased ratio of calretinin-positive dendrites can be also explained by the degeneration of calretinin-positive profiles.

In the case of sclerotic samples, the extensive loss of the majority of natural targets (calretinin-positive interneurons and pyramidal cells) and the presence of resistant interneurons may cause the shift of the target distribution to higher proportions of interneuron-like profiles.

Calretinin-immunoreactive interneuron-specific cells may participate in the synchronization of dendritic inhibitory interneurons (Gulyas et al., 1996; Magloczky and Freund, 2005), the concerted action of which is necessary to control dendritic electrogenesis (Miles et al., 1996) and synaptic plasticity. This hypothesis is
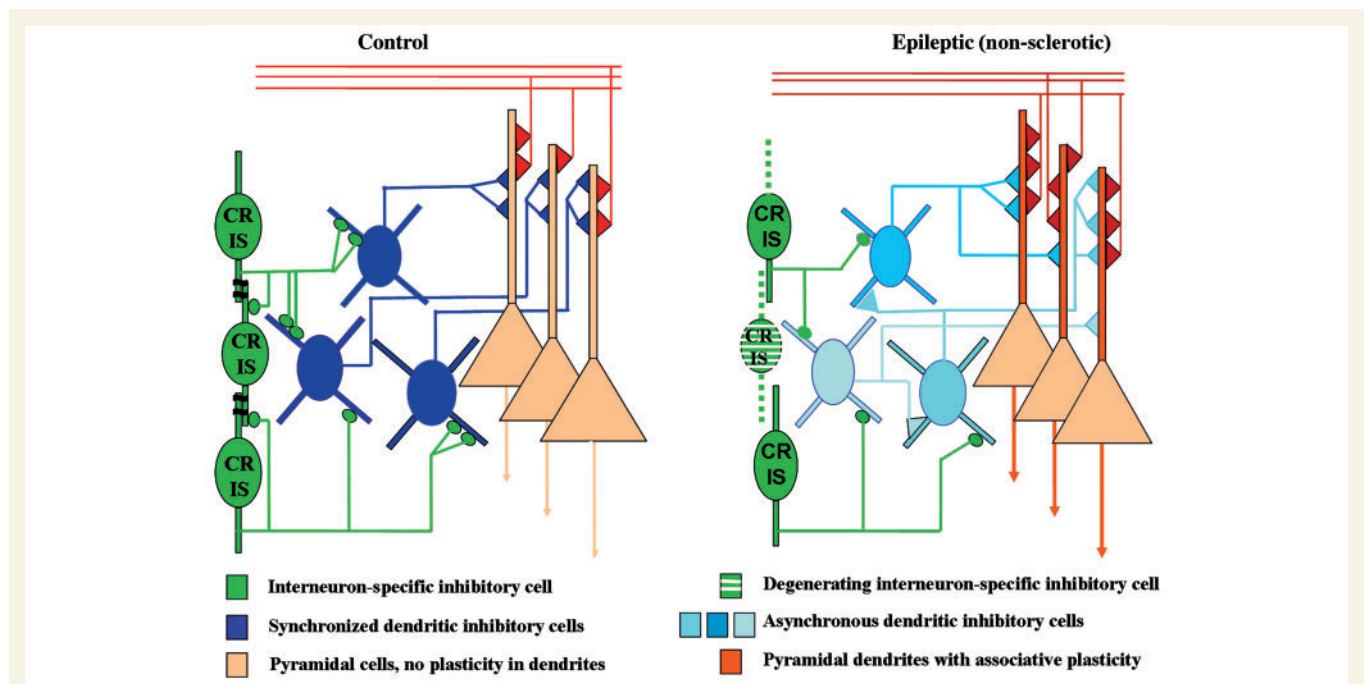

Figure 8 Summary diagram of the inhibitory synaptic reorganization involving calretinin-immunoreactive cells and dendritic inhibitory interneurons in the non-sclerotic epileptic human hippocampus. Control: a part of the calretinin-positive cells are interneuron selective inhibitory cells in the human hippocampus targeting dendritic inhibitory cells and other calretinin-containing interneurons (green). Calretinin-containing neurons also form dendro-dendritic contacts with each other. The electrically coupled calretinin-positive cells can efficiently synchronize the action of dendritic inhibitory cells (dark blue) on pyramidal cell dendrites (orange). Epileptic, non-sclerotic: some calretinin-positive cells are degenerated resulting in an impairment of the calretinin-positive interneuron ensemble. This may lead to the asynchronous firing of the targeted dendritic inhibitory cells (light blue) which may cause a less effective inhibition of pyramidal cell dendrites. This may result in abnormally enhanced potentiation of excitatory inputs to principal cells.

supported by our finding that calbindin-containing dendritic inhibitory interneurons are targeted by calretinin-positive interneuron terminals both in control and epileptic hippocampi (Fig. 7).

Our results show that both synaptic and dendro-dendritic contacts of calretinin-positive interneurons are impaired even in the non-sclerotic cases, where the majority of principal and non-principal cells are preserved. The dendritic tree of calretinin-immunoreactive cells is damaged, which may result in impaired synchronization of the calretinin-positive cell ensemble and consequently of the entire interneuron network responsible for dendritic inhibition. This may lead to an inefficient control of the efficacy and plasticity of excitatory inputs to pyramidal cells (Fig. 8), and subsequently to the formation of principal cell assemblies connected by abnormally potentiated synapses, which may be involved in epileptogenesis and seizure generation.

This may partly explain why severe intractable seizures occur in non-sclerotic patients, where the majority of principal and non-principal cells are preserved. Non-sclerotic patients have abnormal interneuronal networks with intact output from the CA1 region (with the preservation of most CA1 pyramidal cells), which may create a potent epileptogenic region.

Acknowledgements

Funding

References

Abraham H, Meyer G. Reelin-expressing neurons in the postnatal and adult human hippocampal formation. Hippocampus 2003; 13: 715–27.

Amaral DG, Cowan WM. Subcortical afferents to the hippocampal formation in the monkey. J Comp Neurol 1980; 189: 573–91.

Andre V, Marescaux C, Nehlig A, Fritschy JM. Alterations of hippocampal GABaergic system contribute to development of spontaneous recurrent seizures in the rat lithium-pilocarpine model of temporal lobe epilepsy. Hippocampus 2001; 11: 452–68.

Babb TL, Pretorius JK, Kupfer WR, Crandall PH. Glutamate decarboxylase-immunoreactive neurons are preserved in human epileptic hippocampus. J Neurosci 1989; 9: 2562–74.

Baimbridge KG, Miller JJ. Immunohistochemical localization of calcium-binding protein in the cerebellum, hippocampal formation and olfactory bulb of the rat. Brain Res 1982; 245: 223–9.

Blumcke I, Beck H, Nitsch R, Eickhoff C, Scheffler B, Celio MR, et al. Preservation of calretinin-immunoreactive neurons in the hippocampus of epilepsy patients with Ammon's horn sclerosis. J Neuropathol Exp Neurol 1996; 55: 329–41.

Blumcke I, Beck H, Suter B, Hoffmann D, Fodisch HJ, Wolf HK, et al. An increase of hippocampal calretinin-immunoreactive neurons correlates with early febrile seizures in temporal lobe epilepsy. Acta Neuropathol 1999; 97: 31–9.

Bokor H, Csaki A, Kocsis K, Kiss J. Cellular architecture of the nucleus reuniens thalami and its putative aspartatergic/glutamatergic projection to the hippocampus and medial septum in the rat. Eur J Neurosci 2002; 16: 1227–39.

Cossart R, Dinocourt C, Hirsch JC, Merchan-Perez A, De Felipe J, Ben-Ari Y, et al. Dendritic but not somatic GABAergic inhibition is decreased in experimental epilepsy. Nat Neurosci 2001; 4: 52–62.

de Lanerolle NC, Kim JH, Robbins RJ, Spencer DD. Hippocampal interneuron loss and plasticity in human temporal lobe epilepsy. Brain Res 1989; 495: 387–95.

de Lanerolle NC, Kim JH, Williamson A, Spencer SS, Zaveri HP, Eid T, et al. A retrospective analysis of hippocampal pathology in human temporal lobe epilepsy: evidence for distinctive patient subcategories. Epilepsia 2003; 44: 677–87.

de Lanerolle NC, Sloviter RS, Kim JH, Robbins RJ, Spencer DD. Evidence for hippocampal interneuron loss in human temporal lobe epilepsy. Epilepsia 1988; 29: 674.

Esclapez M, Houser CR. Up-regulation of GAD65 and GAD67 in remaining hippocampal GABA neurons in a model of temporal lobe epilepsy. J Comp Neurol 1999; 412: 488–505.

Freund TF, Buzsaki G. Interneurons of the hippocampus. Hippocampus 1996; 6: 347–470.

Freund TF, Magloczky Z. Early degeneration of calretinin-containing neurons in the rat hippocampus after ischemia. Neuroscience 1993; 56: 581–96.

Gulyas AI, Hajos N, Freund TF. Interneurons containing calretinin are specialized to control other interneurons in the rat hippocampus. J Neurosci 1996; 16: 3397–411.

Gulyas AI, Miettinen R, Jacobowitz DM, Freund TF. Calretinin is present in non-pyramidal cells of the rat hippocampus–I. A new type of neuron specifically associated with the mossy fibre system. Neuroscience 1992; 48: 1–27.

Heinrich C, Nitta N, Flubacher A, Muller M, Fahrner A, Kirsch M, et al. Reelin deficiency and displacement of mature neurons, but not neurogenesis, underlie the formation of granule cell dispersion in the epileptic hippocampus. J Neurosci 2006; 26: 4701–13.

Houser CR. GABA neurons in seizure disorders: a review of immunocytochemical studies. Neurochem Res 1991; 16: 295–308.

Houser CR. Neuronal loss and synaptic reorganization in temporal lobe epilepsy. Adv Neurol 1999; 79: 743–61.

Jacobowitz DM, Winsky L. Immunocytochemical localization of calretinin in the forebrain of the rat. J Comp Neurol 1991; 304: 198–218.

Johansen FF, Tonder N, Zimmer J, Baimbridge KG, Diemer NH. Short-term changes of parvalbumin and calbindin immunoreactivity in the rat hippocampus following cerebral ischemia. Neurosci Lett 1990; 120: 171–4.

Kosaka T, Hama K. Gap junctions between non-pyramidal cell dendrites in the rat hippocampus (CA1 and CA3 regions): a combined Golgi-electron microscopy study. J Comp Neurol 1985; 231: 150–61.

Loup F, Wieser HG, Yonekawa Y, Aguzzi A, Fritschy JM. Selective alterations in GABAA receptor subtypes in human temporal lobe epilepsy. J Neurosci 2000; 20: 5401–19.

Magloczky Z, Freund TF. Selective neuronal death in the contralateral hippocampus following unilateral kainate injections into the CA3 subfield. Neuroscience 1993; 56: 317–35.

Magloczky Z, Freund TF. Delayed cell death in the contralateral hippocampus following kainate injection into the CA3 subfield. Neuroscience 1995; 66: 847–60.

Magloczky Z, Freund TF. Impaired and repaired inhibitory circuits in the epileptic human hippocampus. Trends Neurosci 2005; 28: 334–40.

Magloczky Z, Wittner L, Borhegyi Z, Halasz P, Vajda J, Czirjak S, et al. Changes in the distribution and connectivity of interneurons in the epileptic human dentate gyrus. Neuroscience 2000; 96: 7–25.

Megias M, Emri Z, Freund TF, Gulyas AI. Total number and distribution of inhibitory and excitatory synapses on hippocampal CA1 pyramidal cells. Neuroscience 2001; 102: 527–40.

Miettinen R, Gulyas AI, Baimbridge KG, Jacobowitz DM, Freund TF. Calretinin is present in non-pyramidal cells of the rat hippocampus–II. Co-existence with other calcium binding proteins and GABA. Neuroscience 1992; 48: 29–43.

Miles R, Toth K, Gulyas AI, Hajos N, Freund TF. Differences between somatic and dendritic inhibition in the hippocampus. Neuron 1996; 16: 815–23.

Muller MC, Osswald M, Tinnes S, Haussler U, Jacobi A, Forster E, et al. Exogenous reelin prevents granule cell dispersion in experimental epilepsy. Exp Neurol 2009; 216: 390–7.

Nitsch R, Ohm TG. Calretinin immunoreactive structures in the human hippocampal formation. J Comp Neurol 1995; 360: 475–87.

Resibois A, Rogers JH. Calretinin in rat brain – an immunohistochemical study. Neuroscience 1992; 46: 101–34.

Seress L, Gulyas AI, Ferrer I, Tunon T, Soriano E, Freund TF. Distribution, morphological features, and synaptic connections of parvalbumin- and calbindin D28k-immunoreactive neurons in the human hippocampal formation. J Comp Neurol 1993a; 337: 208–30.

Seress L, Gulyas AI, Freund TF. Parvalbumin- and calbindin D28k-immunoreactive neurons in the hippocampal formation of the macaque monkey. J Comp Neurol 1991; 313: 162–77.

Seress L, Gulyas AI, Freund TF. Pyramidal neurons are immunoreactive for calbindin D28k in the CA1 subfield of the human hippocampus. Neurosci Lett 1992; 138: 257–60.

Seress L, Nitsch R, Leranth C. Calretinin immunoreactivity in the monkey hippocampal formation–I. Light and electron microscopic characteristics and co-localization with other calcium-binding proteins. Neuroscience 1993b; 55: 775–96.

Shan W, Yoshida M, Wu XR, Huntley GW, Colman DR. Neural (N-) cadherin, a synaptic adhesion molecule, is induced in hippocampal mossy fiber axonal sprouts by seizure. J Neurosci Res 2002; 69: 292–304.

Slezia A, Kekesi AK, Szikra T, Papp AM, Nagy K, Szente M, et al. Uridine release during aminopyridine-induced epilepsy. Neurobiol Dis 2004; 16: 490–9.

Sloviter RS, Sollas AL, Barbaro NM, Laxer KD. Calcium-binding protein (calbindin-D28K) and parvalbumin immunocytochemistry in the normal and epileptic human hippocampus. J Comp Neurol 1991; 308: 381–96.

Spencer DD, Spencer SS. Surgery for epilepsy. Neurol Clin 1985; 3: 313–30.

Suckling J, Roberts H, Walker M, Highley JR, Fenwick P, Oxbury J, et al. Temporal lobe epilepsy with and without psychosis: exploration of hippocampal pathology including that in subpopulations of neurons defined by their content of immunoreactive calcium-binding proteins. Acta Neuropathol 2000; 99: 547–54.

Sundstrom LE, Brana C, Gatherer M, Mepham J, Rougier A. Somatostatin- and neuropeptide Y-synthesizing neurones in the fascia dentata of humans with temporal lobe epilepsy. Brain 2001; 124: 688–97.

Tang FR, Chia SC, Jiang FL, Ma DL, Chen PM, Tang YC. Calcium binding protein containing neurons in the gliotic mouse hippocampus with special reference to their afferents from the medial septum and the entorhinal cortex. Neuroscience 2006; 140: 1467–79.

Thom M, Sisodiya SM, Beckett A, Martinian L, Lin WR, Harkness W, et al. Cytoarchitectural abnormalities in hippocampal sclerosis. J Neuropathol Exp Neurol 2002; 61: 510–9.

Toth K, Wittner L, Urban Z, Doyle WK, Buzsaki G, Shigemoto R, et al. Morphology and synaptic input of substance P receptor-immunoreactive interneurons in control and epileptic human hippocampus. Neuroscience 2007; 144: 495–508.

Urban Z, Magloczky Z, Freund TF. Calretinin-containing interneurons innervate both principal cells and interneurons in the CA1 region of the human hippocampus. Acta Biol Hung 2002; 53: 205–20.

van Vliet EA, Aronica E, Tolner EA, Lopes da Silva FH, Gorter JA. Progression of temporal lobe epilepsy in the rat is associated with immunocytochemical changes in inhibitory interneurons in specific regions of the hippocampal formation. Exp Neurol 2004; 187: 367–79.

Wittner L, Eross L, Czirjak S, Halasz P, Freund TF, Magloczky Z. Surviving CA1 pyramidal cells receive intact perisomatic inhibitory input in the human epileptic hippocampus. Brain 2005; 128: 138–52.

Wittner L, Eross L, Szabo Z, Toth S, Czirjak S, Halasz P, et al. Synaptic reorganization of calbindin-positive neurons in the human hippocampal CA1 region in temporal lobe epilepsy. Neuroscience 2002; 115: 961–78.

Wittner L, Magloczky Z, Borhegyi Z, Halasz P, Toth S, Eross L, et al. Preservation of perisomatic inhibitory input of granule cells in the epileptic human dentate gyrus. Neuroscience 2001; 108: 587–600.